Oct 26th, 12:00 AM

Impact of Holes on the Elastic Buckling of Cold-formed Steel Columns

Christopher D. Moen

Benjamin W. Schafer

Eighteenth International Specialty Conference on Cold-Formed Steel Structures
Orlando, Florida, USA, October 26 & 27, 2006

Impact of Holes on the Elastic Buckling of Cold-Formed Steel Columns with Application to the Direct Strength Method

Cristopher D. Moen[1], Benjamin W. Schafer[2]

Abstract

The objective of the research presented in this paper is to develop an extension to the Direct Strength Method for predicting the strength of cold-formed steel members containing holes. This paper represents the first stage toward the research objective and focuses on the elastic buckling behavior of plates and cold-formed steel channel compression members containing a single perforation. A parametric study evaluates the effect of a slotted web hole on the elastic buckling behavior of seven Steel Stud Manufacturer's Association (SSMA) structural stud sections. The general purpose finite element code ABAQUS is used to calculate the elastic buckling behavior of these structural studs, which is then compared to simply supported plate models of the stud webs. The addition of a hole changes the length and number of local buckling half-waves in both the member and plate models. A correlation between increased elastic buckling load and changing buckling wavelength is observed. Another parametric study evaluates the effect of circular hole diameter on the elastic buckling load and mode shapes of an SSMA 362S162-33 structural stud. Several new mixed local, distortional, and global buckling modes are created by the addition of the hole, some of which have elastic buckling loads significantly lower than a member without a hole. An examination of the ultimate strength of compression members with holes is conducted. First the elastic buckling behavior of stub column and long column specimens from five experimental programs is determined. This information is then used to calculate the predicted compressive strengths through an extension of the Direct Strength Method (DSM). Favorable comparisons are made between tested specimen strengths and predicted DSM strengths.

[1] Graduate Research Assistant, Johns Hopkins University, Baltimore, MD, 21218, USA. (moen@jhu.edu)
[2] Assistant Professor, Johns Hopkins University, Baltimore, MD, 21218, USA. (schafer@jhu.edu)

Introduction

Many cold-formed steel compression members contain prepunched perforations. For example, filleted rectangular web holes are provided in structural channel studs to accommodate utilities. Also, hole patterns are punched into storage rack columns to accommodate shelving units. The current North American Cold-Formed Steel Design Specification (NAS 2001) provides two methods for predicting the strength of cold-formed steel compression members with holes. Section B2.2 of the Specification presents a strength prediction method for members with circular holes based on the work of Ortiz-Colberg (1981). A method for non-circular holes is described in Section D4 of the Specification and utilizes the "unstiffened strip" approach developed by Miller and Peköz (1989, 1994). The "unstiffened strip" approach calculates the effective width of a plate with a hole by idealizing the area around the hole as two long plates simply supported on three sides and free on the edge adjacent to the hole. These strength prediction methods can only be applied to certain cross sections and are only valid for specific hole locations, hole spacings, and hole sizes. It is also common that requests for field cut holes exceed the predefined limits of these methods.

This paper presents initial work toward extending the Direct Strength Method (DSM) to members with holes. DSM is a design methodology which uses member elastic buckling behavior in conjunction with experimentally established post-buckling trends to predict ultimate strength (NAS 2004 Appendix 1, Schafer and Peköz 1998). When predicting the compressive strength of columns, DSM requires an estimation of the elastic buckling loads in local, distortional, and global buckling modes. Therefore, extension of DSM to members with holes begins by evaluating the effect of holes on the elastic buckling loads of cold-formed steel members.

Two elastic buckling parameter studies are presented in this paper, the first evaluates the effect of a slotted web hole on the elastic buckling behavior of Steel Stud Manufacturer's Association (SSMA) structural stud sections, and the second evaluates the effect of circular hole diameter on the elastic buckling load and mode shapes of an SSMA 362S162-33 structural stud. The ultimate strength of stub column and long column specimens with holes is evaluated by comparing DSM predictions to the tested strengths of five experimental programs conducted between 1981 and 1999.

Dimension Nomenclature

The member and hole dimension nomenclature used in this paper is summarized in Figure 1.

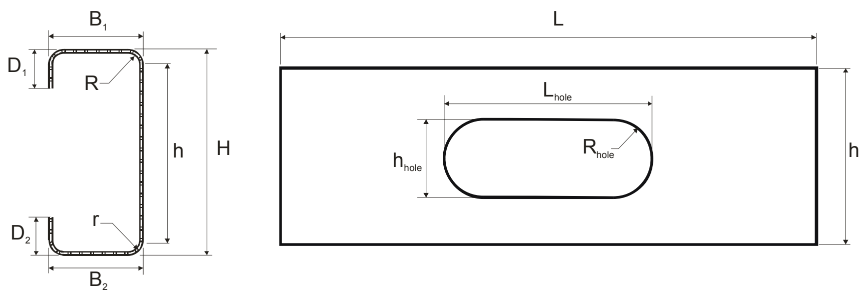

Figure 1. Channel and hole dimension nomenclature

Elastic Buckling Predictions

Finite Element Modeling

The elastic buckling behavior of the plates and structural studs in this section are obtained with an eigenbuckling analysis in ABAQUS (ABAQUS 2004). All members are modeled with S9R5 reduced integration nine-node thin shell elements. Plate boundary conditions are modeled as simply supported. Structural stud boundary conditions are modeled as warping free at the member ends and warping fixed at the midlength of the member, which mimics the semi-analytical finite strip method. Both plates and structural studs are loaded from each end with a uniform compressive stress applied as consistent nodal loads in ABAQUS. Cold-formed steel material properties are assumed as E=203 GPa and v=0.3. Element meshing was performed using purpose-built MATLAB (Mathworks 2005) code written by the first author.

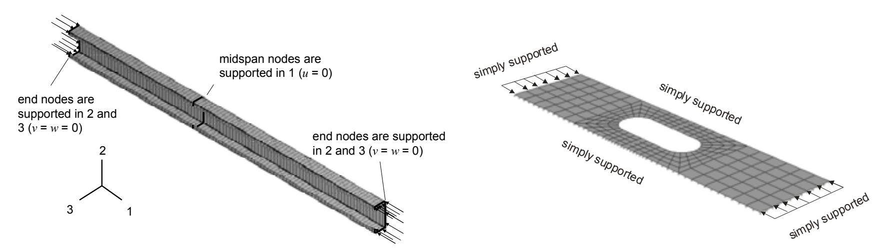

Figure 2. Boundary and loading conditions assumed in ABAQUS

Elastic Stability of Plates with an Isolated Hole

This study evaluates the influence of one slotted hole on the elastic buckling behavior of a range of rectangular plates and SSMA cold-formed steel structural stud sections. The slotted hole has dimensions of h_{hole}=38.1 mm, L_{hole}=101.6 mm, and R_{hole}=19.1 mm. The plate widths are chosen to correspond with the flat web widths of standard SSMA structural studs. Plate aspect ratios are held constant at 4:1. From each plate, a full structural stud finite element model is also developed for comparison. The SSMA member designations and cross section dimensions considered in this study are listed in Table 1.

Table 1 Structural Stud and Plate Dimensions

SSMA Designation	H (mm)	B1 (mm)	B2 (mm)	D1 (mm)	D2 (mm)	R (mm)	t (mm)	r (mm)	h (mm)	h_{hole}/h	L=4h (mm)
250S162-33	63.5	41.3	41.3	12.7	12.7	1.9	0.88	2.38	57.9	0.66	231
350S162-33	88.9								83.3	0.46	333
362S162-33	91.9								86.3	0.44	345
400S162-33	101.6								96.0	0.40	384
550S162-33	139.7								134.1	0.28	536
600S162-33	152.4								146.8	0.26	587
800S162-33	203.2	↓*	↓	↓	↓	↓	↓	↓	197.6	0.19	790

* → denotes number repeats

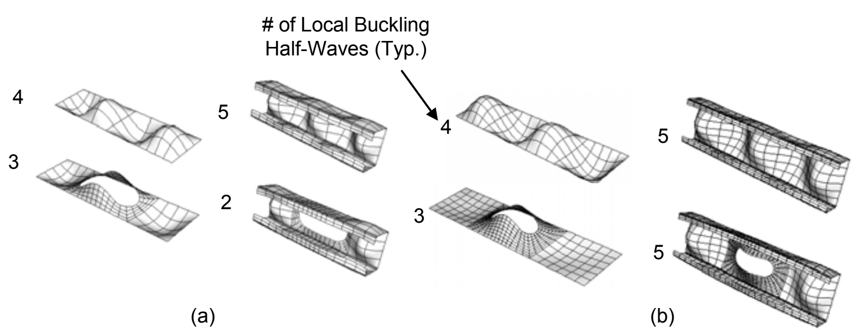

(a) SSMA 250S162-33 h_{hole}/h=0.66

(b) SSMA 400S162-33 h_{hole}/h=0.40

Figure 3. (a) SSMA 250S162-33 web plate and structural stud, and (b) SSMA 400S162-33 web plate and structural stud

Before examining the elastic buckling load, consider the observed changes in the first mode shape caused by the addition of a hole as given in Figure 3. For the buckled shape of the SSMA 250S162-33 in Figure 3a, the number of buckled half-waves changes from four to three for the isolated plate and from five to two for the full member, when the hole is added. Corresponding to the decreased number of half-waves is an increase in the buckling half-wavelength. In Figure 3b, the hole decreases the number of buckled half-waves from four to three in the SSMA 440S162-33 isolated plate but does not change the number of half-waves in the full member.

A rectangular plate loaded in uniform compression with an aspect ratio of 4:1 will buckle into four half-waves at a load P_{cr} as shown in Figure 4a. The natural wavelength is equal to the width of the plate, and this corresponds to the lowest energy required to initiate buckling. Consider a plate with a hole, where the presence of the hole has changed the number of half-waves from four to three as shown in Figure 4b. In the locally buckled cells without the hole the wavelength has increased above the natural wavelength, which effectively increases P_{cr} in this region. This is termed the wavelength stiffening effect. In the locally buckled cell that includes the hole the buckling behaves more like an "unstiffened strip" and P_{cr} is generally decreased (for $h_{hole}/h<0.57$) though for large holes P_{cr} may be increased as well. This is termed the "unstiffened strip" effect. The actual P_{cr} for the entire plate with the hole is a combination of the wavelength stiffening effect (always beneficial) and the "unstiffened strip" effect (can be beneficial or detrimental depending on hole size).

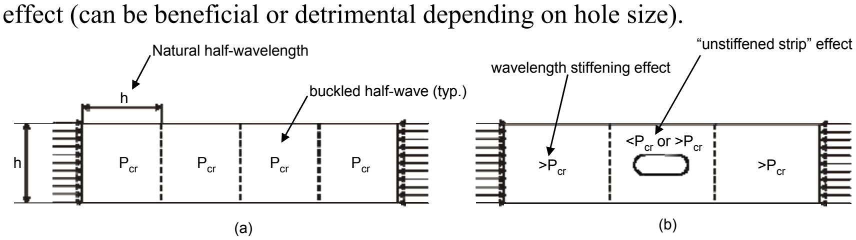

Figure 4. Influence of a hole on local buckling wavelengths and elastic buckling load P_{cr}

Figure 5 presents the elastic buckling loads of the isolated web plates and full members with holes of Table 1. These results are compared to a modified "unstiffened strip" approximation which assumes that P_{cr} of the plate with a hole is equal to the elastic buckling stress f_{cr} of the web strip adjacent to the hole multiplied by the net area of the plate. For small hole width to plate width ratios, the buckling load of the isolated plates is as much as 70 percent higher than the modified "unstiffened strip" approximation. This increase is attributed to the change in buckled half-wavelength created by the hole. As normalized hole width increases, the elastic buckling load exceeds that of a plate without a hole. This increase in buckling load is attributed to a combination of wavelength stiffening and "unstiffened strip" effects. Similar trends for rectangular plates with circular holes are observed by El-Sawy and Nazmy (2001).

The structural stud results in Figure 5 demonstrate that the addition of flanges and lip stiffeners to the isolated web plates increase the elastic buckling load. The web is stiffened through beneficial web-flange interaction created by the relatively stable edge-stiffened flange. The increase in buckling load of the structural studs with the addition of a hole is attributed to a combination of the previously discussed wavelength stiffening effect and "unstiffened strip" effect.

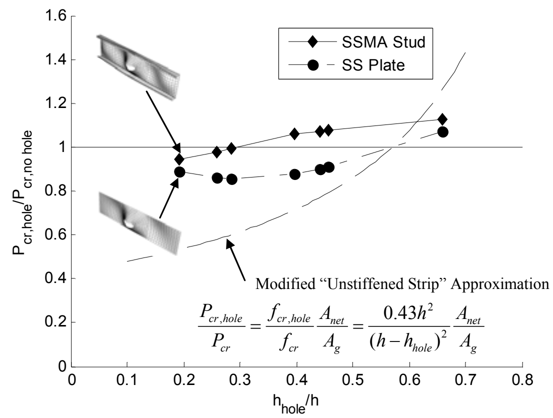

Figure 5. Effect of a slotted hole on the elastic buckling load of simply supported plates and structural studs

Structural Stud Mode Shape and Hole Size Study

This study evaluates the influence of circular hole diameter on the elastic buckling behavior of an intermediate length SSMA 362S162-33 structural stud. A single hole was placed at the midlength of the stud web and centered between the flanges. Five hole diameters were considered, h_{hole}/h=0.1, 0.3, 0.5, 0.7, and 0.9 where the flat web width h=86.3 mm. The length L is 1220 mm for all members.

The first task in this study was to identify and group buckled mode shapes using existing definitions for local (L), distortional (D), and global buckling (G) described in the DSM commentary (NAS 2004 Appendix 1). Figure 6 summarizes the common mode shapes observed in this identification phase and compares them to the mode shapes of the same member, but without a hole. For local buckling, the mode shapes are similar for members with and without holes except that local web buckling deformations are dampened near the hole. The distortional mode shape takes on a local mixed component when the hole is added, but the buckling load is not significantly affected. The global flexural-torsional mode shape is not affected by the size of hole for this member.

The addition of the hole creates at least two new relevant buckled shapes, the DH+L and DH2 modes, which are also presented in Figure 6. The DH+L mode is a mixed mode where distortional buckling near the hole combines with local web and flange buckling. The DH2 mode is an isolated hole mode where antisymmetric distortional buckling of the flanges occurs at the hole. This type of antisymmetric mode exists in members without holes, although typically its elastic buckling load is higher than the primary distortional mode and is not considered in a typical design.

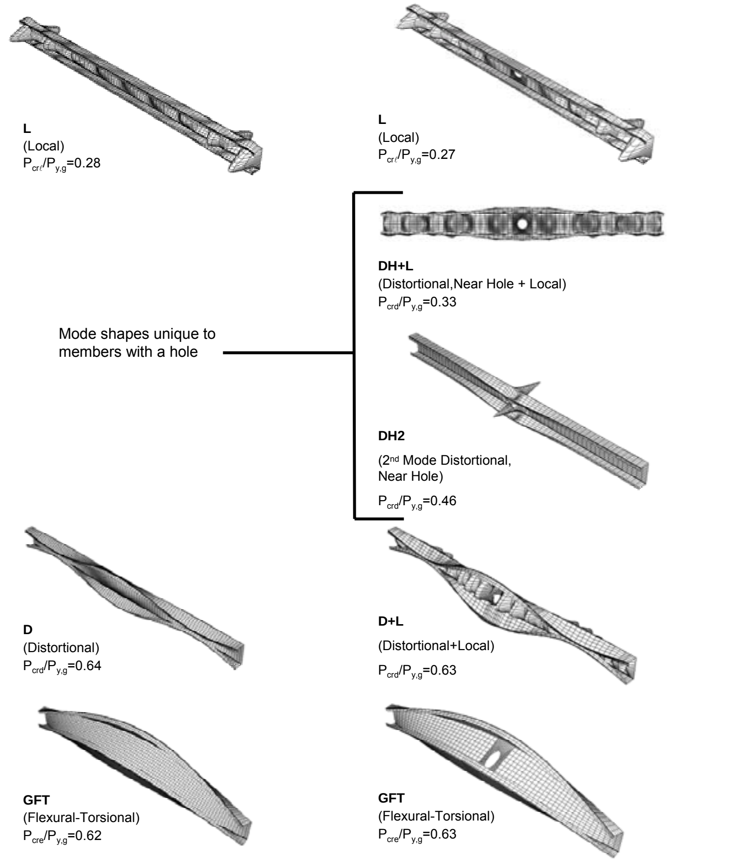

Figure 6. Buckling mode shape summary, 362S162-33 channel with circular hole, L=1220 mm, hole diameter to flat web width ratio of 0.5

Figure 7 presents the elastic buckling loads of the buckled shapes in Figure 6 as a function of normalized hole diameter. For the member length and cross-section chosen in this study, the local, distortional, and global buckling elastic loads are not significantly affected by the circular hole, even at large diameters. However, the DH+L buckling load decreases with increasing hole diameter and converges to the local buckling load at h_{hole}/h=0.9. This trend is significant because it suggests that the DH+L mode is important when predicting the compressive strength of the structural stud. It is also noted that the DH2 mode has an elastic buckling load lower than the primary distortional mode D when h_{hole}/h is between 0.3 and 0.7, suggesting that it also may play a role in the compressive strength of this structural stud. The DH+L and DH2 modes are expected to be even more important when predicting the strength of sections where the distortional buckling load is already less than the local buckling load, such as some beams and rack posts, for example.

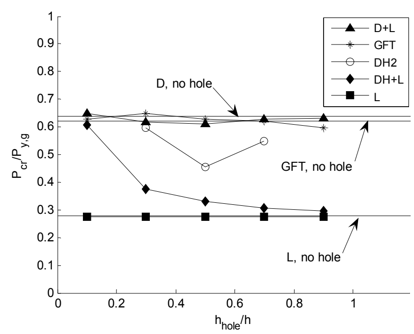

Figure 7. Influence of circular hole diameter on the elastic buckling of a SSMA 362S162-33 structural stud

Elastic Buckling Loads of Stub Column and Long Column Test Specimens

Test specimens from five experimental programs, listed in Table 2, are modeled in ABAQUS to determine their elastic buckling behavior. The data set is made up of cold-formed steel stub column and long column lipped channel specimens containing a single web hole at the specimen midlength and centered between the flanges. Table A-1 and A-2 of the Appendix summarize the stub column and long column cross-section and hole dimensions, tested ultimate load, $P_{test,}$ and specimen yield force, $P_{y,g}$ (calculated with the gross cross sectional area). Member boundary and loading conditions are modeled consistent with the experimental conditions summarized in Table 2.

Table 2 Summary of Experimental Programs Considered

Reference	Author	Publication Date	Types of Specimens	Cross Section	End Conditions
1	Ortiz-Colberg	1981	Stub Column Long Column	Lipped Channel	Fixed-Fixed Weak Axis Pinned
2	Miller and Peköz	1994	Stub Column	Lipped Channel	Fixed-Fixed
3	Sivakumaran	1987	Stub Column	Lipped Channel	Fixed-Fixed
4	Abdel-Rahman	1997	Stub Column	Lipped Channel	Fixed-Fixed
5	Pu et al.	1999	Stub Column	Lipped Channel	Fixed-Fixed

For each specimen the local, distortional, and global buckling modes are manually identified from the buckled modes determined in the ABAQUS eigenbuckling analysis. For example, the buckled shapes of stub column specimen A8 (Sivakumaran 1987) are presented in Figure 8. The L and DH+L elastic buckling loads are similar, suggesting that distortional buckling will influence the compressive strength of this member. The web adjacent to the hole is restrained by the flanges in the local L mode, causing the web to buckle in two half-waves. In the DH+L mode, the distortion of the flanges allows the web at the hole to buckle as a single half-wave.

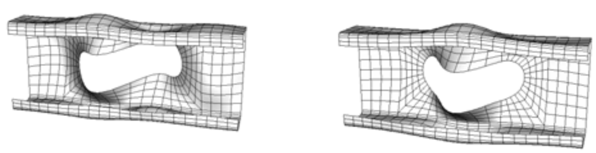

L
(Local)
$P_{cr\ell}/P_{y,g}$=1.31

DH+L
(Distortional,Near Hole + Local)
$P_{crd}/P_{y,g}$=1.34

Figure 8. Buckled Mode Shapes for Specimen A8, Sivakumaran 1987

The elastic buckling loads for the local mode of all stub column specimens are plotted in Figure 9 as a function of hole width to flat web width. The local buckling load for most stub column specimens is equal to or higher than the local buckling load without a hole, and exhibits a general increasing trend with increasing normalized hole width. It is postulated that the increase in local buckling loads with the addition of a hole is a caused by a combination of the wavelength stiffening and "unstiffened strip" effects discussed in the previous section of this paper.

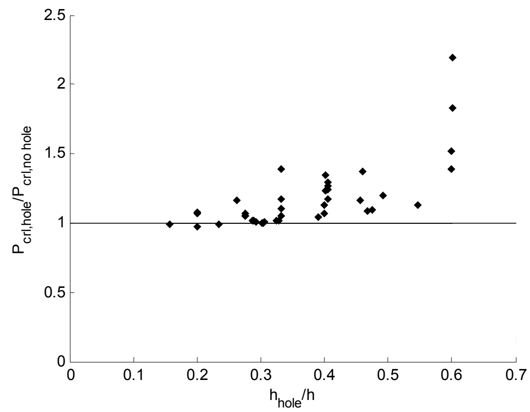

Figure 9. Influence of hole width on stub column local buckling load

Figure 10 demonstrates the influence of a hole on the distortional buckling load of the stub column specimens considered in this study. It is observed that in most cases the mixed distortional and local modes DH+L and DH2 have elastic buckling loads significantly less than that of the distortional modes typically considered in design. Also, simple predictions of the DH2 and DH+L buckling loads using h_{hole}/h are not possible. Similar distortional buckling trends are observed for the long column specimens.

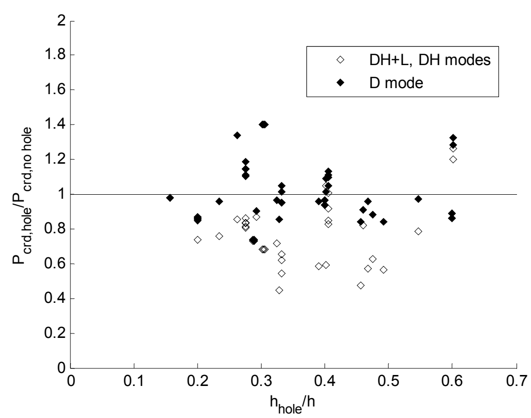

Figure 10. Influence of hole width on stub column distortional buckling load

Figure 11 compares the distortional buckling behavior of long column Specimen L10 (Ortiz-Colberg 1981) with and without a hole. The pure distortional mode D becomes a mixed mode D+L when the hole is added. Two additional modes are also created, DH+L and DH2, both having buckling loads less than that of the member without a hole. This result is consistent with the circular hole study trends in Figure 7 and again demonstrates how a hole can potentially affect the strength of this type of compression member.

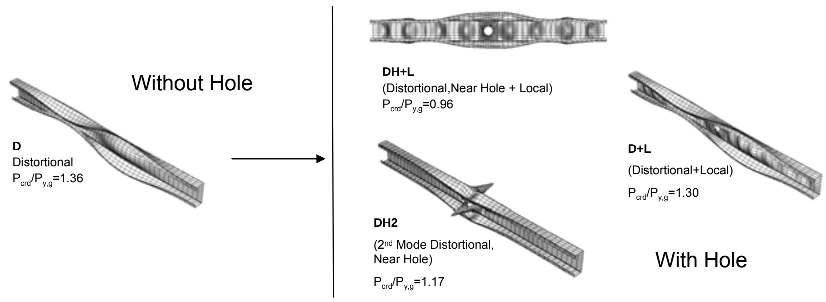

Figure 11 Distortional Mode Shapes for Specimen L10, Ortiz-Colberg 1981

Tested vs. Predicted Ultimate Strength Using the Direct Strength Method

In this section the tested ultimate compressive strengths of the specimens from the five experimental programs described in Table 2 are now compared to the Direct Strength Method (DSM) predictions. The basic premise of the Direct Strength Method is expressed for a column as $P_n=f(P_{cr\ell}, P_{crd}, P_{cre}, P_y)$ where P_n is the nominal column strength, P_y is the axial load at yielding, and $P_{cr\ell}$, P_{crd}, P_{cre} are the axial loads at which elastic local, distortional, and global (flexural, torsional, flexural-torsional) buckling occur (NAS 2004 Appendix 1). $P_{cr\ell}$, P_{crd}, P_{cre} are obtained from the results described in the *Elastic Buckling* section of this paper. For both stub column and long column specimens, P_{crd} is conservatively chosen as the minimum buckling load from the DH+L, DH2, and D modes. P_y is calculated using the gross cross sectional area A_g (Moen and Schafer 2006).

Figure 12 compares the tested ultimate compressive strengths of the stub column specimens with the DSM local and distortional prediction curves. The local buckling controlled specimens generally follow the DSM prediction curve. For specimens controlled by distortional buckling, the tested strengths exhibit a trend that is slightly different from the DSM prediction curve.

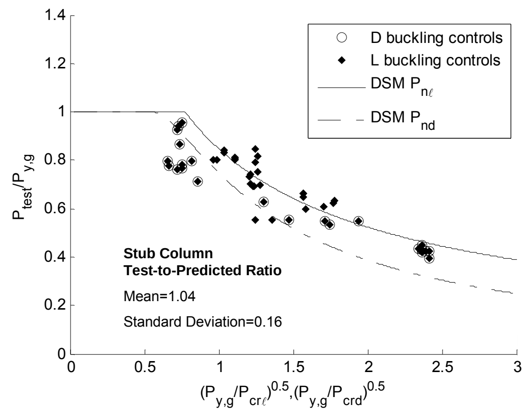

Figure 12. Comparison of stub column tested and predicted ultimate strengths

The long column specimen tested and predicted ultimate strengths are presented in Figure 13. The predicted strengths for specimens controlled by weak axis flexural buckling are generally conservative when compared to the tested strengths. Long column strengths not controlled by this global buckling mode are then dictated by their local buckling loads; for these cases $P_{n\ell}< P_{ne}$ in DSM. The local buckling inset presented in Figure 13 demonstrates that when $P_{n\ell}<P_{ne}$ the specimen tested strengths are generally conservative as compared to DSM predictions.

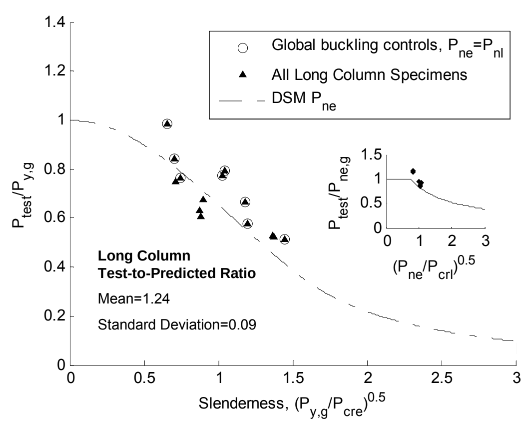

Figure 13. Comparison of long column tested and predicted ultimate strengths

Conclusions

The first steps have been taken toward developing an extension to the Direct Strength Method (DSM) for predicting the strength of cold-formed steel members with holes. This paper focuses on the elastic buckling behavior of flat plates and cold-formed steel structural channel studs. Also, stub column and long column specimen strengths are compared to DSM predictions.

Elastic Buckling

Holes are generally assumed to decrease the elastic local buckling load of a flat plate loaded in uniform compression; however, the hole often causes a change in the wavelength of the buckling mode which actually increases the buckling load away from the hole. Mixed local, distortional, and global buckling modes are created when a hole is placed in the web of an intermediate length structural stud. Distortional buckling at the location of the hole (DH+L) is common and occurs at an elastic buckling load less than that of a pure distortional mode. As the hole width increases relative to the web width, the DH+L buckling load approaches the local buckling load for the member. The global buckling load of an intermediate length structural stud is not affected by a hole with the boundary conditions and hole location considered in this study.

Tested vs. Predicted Ultimate Strength Using the Direct Strength Method

For the stub column channel specimens controlled by local buckling, the DSM predictions are generally consistent with tested strengths. When distortional buckling controls, the stub column tested strengths exhibited a slightly different (overly conservative) trend than the DSM prediction curve. The tested strengths of long column channel specimens were generally conservative when compared to DSM predictions that have elastic buckling loads which accurately include the influence of the hole.

Acknowledgements

The sponsorship of the American Iron and Steel Institute is gratefully acknowledged. Thanks to Johns Hopkins undergraduate Matt McCarty for his contributions to this research. Visiting scholar Jaswant Arlekar also contributed to early studies in this work.

Appendix - References

ABAQUS (2004). *ABAQUS/Standard Users Manual version 6.4*. ABAQUS, Inc., www.abaqus.com, Providence, RI.

Abdel-Rahman, N. (1997). Cold-Formed Steel Compression Members with Perforations. PhD Thesis, McMaster University, Hamilton, Ontario, Canada.

El-Sawy, K. M., Nazmy, A. S. (2001). "Effect of aspect ratio on the elastic buckling of uniaxially loaded plates with eccentric holes." *Thin-Walled Structures*, 39(12), 983-998.

Mathworks (2006). *MATLAB version 7*. Mathworks, Inc., www.mathworks.com, Natick, MA.

Miller, T.H., Peköz, T. (1989). "Studies on the behavior of cold-formed steel wall stud assemblies." Final Report, Cornell University, Ithaca, NY.

Miller, T.H., Peköz, T. (1994). "Unstiffened strip approach for perforated wall studs." *Journal of Structural Engineering*, ASCE, Vol. 120, No. 2.

Moen, C., Schafer, B.W. (2006). "Direct strength design for cold-formed steel members with perforations." *Progress Report*, American Iron and Steel Institute, Washington, D.C.

North American Specification (NAS). (2001). *North American Specification for the Design of Cold-Formed Steel Structural Members*, American Iron and Steel Institute. Washington, D.C.

North American Specification (NAS). (2004). *2004 Supplement to the North American Specification for the Design of Cold-Formed Steel Structures*. American Iron and Steel Institute, Washington, D.C.

Ortiz-Colberg, R. A. (1981). The Load Carrying Capacity of Perforated Cold Formed Steel Columns. Ph.D. Thesis, Cornell University, Ithaca, NY.

Pu, Y., Godley, M. H. R., Beale, R. G., Lau, H. H. (1999). "Prediction of ultimate capacity of perforated lipped channels." *Journal of Structural Engineering*, ASCE, 125(5), 510-514.

Schafer, B.W., Peköz, T. (1998). "Direct strength prediction of cold-formed steel members using numerical elastic buckling solutions." *14th Int'l Spec. Conf. on Cold-Formed Steel Structures*, St. Louis, Missouri.

Sivakumaran, K. S. (1987). "Load capacity of uniformly compressed cold-formed steel section with punched web." *Canadian Journal of Civil Engineering*, 14(4), 550-558.

Table A-1 - Stub Column Experimental Data

Study and Specimen Name		Member		Hole Dimensions				Cross Section Dimensions						Yield	Experimental	
		L (mm)	t (mm)	*Type*	L_{hole} (mm)	h_{hole} (mm)	R_{hole} (mm)	H (mm)	B_1 (mm)	B_2 (mm)	D_1 (mm)	D_2 (mm)	R (mm)	$P_{y,g}$ (kN)	$P_{test,1}$ (kN)	$P_{test,2}$ (kN)
Ortiz-Colberg 1981	S4	305	1.2	Circular	19.1	19.1	9.5	89.0	41.1	37.8	12.5	12.8	2.5	74.1	62.9	---
Ortiz-Colberg 1981	S7	305	1.3	Circular	38.1	38.1	19.1	89.2	41.4	37.9	12.7	13.0	2.5	76.9	56.3	---
Ortiz-Colberg 1981	S6	305	1.3	Circular	31.8	31.8	15.9	89.0	41.0	37.7	12.5	12.9	2.5	81.7	61.4	---
Ortiz-Colberg 1981	S8	305	1.3	Circular	44.5	44.5	22.2	89.0	41.0	37.6	12.5	12.8	2.5	81.7	60.5	---
Ortiz-Colberg 1981	S5	305	1.3	Circular	26.4	26.4	13.2	89.0	41.1	37.6	12.5	12.8	2.5	78.9	62.5	---
Ortiz-Colberg 1981	S3	305	1.3	Circular	12.7	12.7	6.4	88.9	41.0	37.5	12.3	12.8	2.5	78.9	64.5	---
Ortiz-Colberg 1981	S14	305	1.9	Circular	26.4	26.4	13.2	89.3	42.5	37.8	12.9	12.8	2.5	114.6	109.4	---
Ortiz-Colberg 1981	S15	305	1.9	Circular	38.1	38.1	19.1	89.3	42.5	37.9	12.9	12.9	2.5	115.1	106.8	---
Abdel-Rahman 1997	A-C	425	1.9	Circular	63.5	63.5	31.8	203.0	41.6	41.6	13.0	13.0	3.8	214.6	114.3	121.5
Abdel-Rahman 1997	A-S	425	1.9	Square	63.5	63.5	---	203.0	41.6	41.6	13.0	13.0	3.8	214.7	114.3	123.8
Abdel-Rahman 1997	A-O	475	1.9	Oval	114.3	63.5	31.8	203.0	41.6	41.6	13.0	13.0	3.8	214.7	117.3	119
Abdel-Rahman 1997	A-R	475	1.9	Rect.	114.3	63.5	---	203.0	41.6	41.6	13.0	13.0	3.8	214.7	111.8	117.3
Abdel-Rahman 1997	B-C	250	1.3	Circular	38.1	38.1	19.1	101.5	41.6	41.6	13.0	13.0	2.5	81.2	58.1	55.3
Abdel-Rahman 1997	B-S	250	1.3	Square	38.1	38.1	---	101.5	41.6	41.6	13.0	13.0	2.5	81.2	59.2	53.6
Abdel-Rahman 1997	B-O	300	1.3	Oval	101.6	38.1	19.1	101.5	41.6	41.6	13.0	13.0	2.5	81.2	57.4	54.8
Abdel-Rahman 1997	B-R	300	1.3	Rect.	101.6	38.1	---	101.5	41.6	41.6	13.0	13.0	2.5	81.2	56.7	57.1
Pu et al. 1999	C-2.0-1-30-1	370	2.0	Square	26.9	26.9	---	100.0	52.0	52.0	16.0	16.0	4.0	134.3	104.9	---
Pu et al. 1999	C-2.0-1-30-2	370	2.0	Square	26.6	26.8	---	100.0	52.0	52.0	16.0	16.0	4.0	101.6	81.2	---
Pu et al. 1999	C-2.0-1-30-3	370	2.0	Square	26.6	26.7	---	100.0	52.0	52.0	16.0	16.0	4.0	104.3	81.3	---
Pu et al. 1999	C-1.2-1-30-1	360	1.2	Square	26.5	26.5	---	98.4	52.0	52.0	16.0	16.0	2.8	51.8	41.6	---
Pu et al. 1999	C-1.2-1-30-2	360	1.2	Square	26.5	26.5	---	98.4	52.0	52.0	16.0	16.0	2.8	51.8	42	---
Pu et al. 1999	C-1.2-1-30-3	360	1.2	Square	26.5	26.4	---	98.4	52.0	52.0	16.0	16.0	2.8	51.8	41.9	---
Pu et al. 1999	C-0.8-1-30-1	360	0.8	Square	26.4	26.5	---	97.6	52.0	52.0	16.0	16.0	2.0	31.0	20.5	---
Pu et al. 1999	C-0.8-1-30-2	360	0.8	Square	26.4	26.4	---	97.6	52.0	52.0	16.0	16.0	2.0	31.0	20.1	---
Pu et al. 1999	C-0.8-1-30-3	360	0.8	Square	26.4	26.5	---	97.6	52.0	52.0	16.0	16.0	2.0	31.0	20.5	---
Sivakumaran 1987	A2	200	1.6	Circular	16.5	16.5	8.3	92.1	41.3	41.3	12.7	12.7	3.2	101.8	85.8	---
Sivakumaran 1987	A3	200	1.6	Square	16.5	16.5	---	92.1	41.3	41.3	12.7	12.7	3.2	101.8	84.7	---
Sivakumaran 1987	A4	200	1.6	Circular	33.0	33.0	16.5	92.1	41.3	41.3	12.7	12.7	3.2	101.8	81.7	---
Sivakumaran 1987	A5	200	1.6	Square	33.0	33.0	---	92.1	41.3	41.3	12.7	12.7	3.2	101.8	81.6	---
Sivakumaran 1987	A6	200	1.6	Circular	49.5	49.5	24.8	92.1	41.3	41.3	12.7	12.7	3.2	101.8	78.1	---
Sivakumaran 1987	A7	200	1.6	Square	49.5	49.5	---	92.1	41.3	41.3	12.7	12.7	3.2	101.8	77.6	---
Sivakumaran 1987	A8	223	1.6	Oval	102.0	38.0	19.0	92.1	41.3	41.3	12.7	12.7	3.2	101.8	72.6	---
Sivakumaran 1987	B2	265	1.3	Circular	29.0	29.0	14.5	152.4	41.3	41.3	12.7	12.7	2.6	84.6	54	---
Sivakumaran 1987	B3	265	1.3	Square	29.0	29.0	---	152.4	41.3	41.3	12.7	12.7	2.6	84.6	53.2	---
Sivakumaran 1987	B4	265	1.3	Circular	58.0	58.0	29.0	152.4	41.3	41.3	12.7	12.7	2.6	84.6	53.4	---
Sivakumaran 1987	B5	265	1.3	Square	58.0	58.0	---	152.4	41.3	41.3	12.7	12.7	2.6	84.6	51	---
Sivakumaran 1987	B6	265	1.3	Circular	87.0	87.0	43.5	152.4	41.3	41.3	12.7	12.7	2.6	84.6	47.1	---
Sivakumaran 1987	B7	265	1.3	Square	87.0	87.0	---	152.4	41.3	41.3	12.7	12.7	2.6	84.6	47	---
Sivakumaran 1987	B8	265	1.3	Oval	102.0	38.0	19.0	152.4	41.3	41.3	12.7	12.7	2.6	84.6	51.6	---
Miller & Pekoz 1994	1-12	276	1.9	Rect.	70.0	41.0	---	92.0	37.0	37.0	12.0	12.0	2.4	121.4	114.5	---
Miller & Pekoz 1994	1-13	276	1.9	Rect.	70.0	41.0	---	92.0	37.0	37.0	12.0	12.0	2.4	120.8	104.8	---
Miller & Pekoz 1994	1-17	456	0.9	Rect.	57.0	40.0	---	152.0	34.0	34.0	8.0	8.0	2.4	61.9	24.3	---
Miller & Pekoz 1994	1-19	456	0.9	Rect.	57.0	40.0	---	152.0	34.0	34.0	8.0	8.0	2.4	61.9	26.2	---
Miller & Pekoz 1994	2-11	276	1.9	Rect.	65.0	38.0	---	92.0	37.0	37.0	12.0	12.0	2.4	123.5	98.7	---
Miller & Pekoz 1994	2-12	276	1.9	Rect.	65.0	38.0	---	92.0	37.0	37.0	12.0	12.0	2.4	123.5	98.3	---
Miller & Pekoz 1994	2-14	456	0.9	Rect.	57.0	40.0	---	152.0	35.0	35.0	8.0	8.0	2.4	61.7	26.6	---
Miller & Pekoz 1994	2-15	456	0.9	Rect.	57.0	40.0	---	152.0	35.0	35.0	8.0	8.0	2.4	61.0	25.9	---
Miller & Pekoz 1994	2-16	456	0.9	Rect.	57.0	40.0	---	152.0	35.0	35.0	8.0	8.0	2.4	61.7	26.0	---
Miller & Pekoz 1994	2-24	456	0.9	Rect.	57.0	40.0	---	152.0	35.0	35.0	8.0	8.0	2.4	62.4	27.0	---
Miller & Pekoz 1994	2-25	456	0.9	Rect.	57.0	40.0	---	152.0	35.0	35.0	8.0	8.0	2.4	62.4	27.0	---
Miller & Pekoz 1994	2-26	456	0.9	Rect.	57.0	40.0	---	152.0	35.0	35.0	8.0	8.0	2.4	61.7	27.8	---

Table A-2 - Long Column Experimental Data

Study and Specimen Name		Member		Hole Dimensions				Cross Section Dimensions						Yield	Exper.
		L (mm)	t (mm)	*Type*	L_{hole} (mm)	h_{hole} (mm)	R_{hole} (mm)	H (mm)	B_1 (mm)	B_2 (mm)	D_1 (mm)	D_2 (mm)	R (mm)	$P_{y,g}$ (kN)	$P_{test,1}$ (kN)
Ortiz-Colberg 1981	L2	1600	1.2	Circular	12.7	12.7	6.4	89.2	41.2	37.7	12.7	12.9	2.5	71.9	37.8
Ortiz-Colberg 1981	L3	686	1.2	Circular	25.4	25.4	12.7	89.2	41.2	37.7	12.7	12.9	2.5	67.5	50.5
Ortiz-Colberg 1981	L6	1600	1.2	Circular	25.4	25.4	12.7	89.2	41.2	37.7	12.7	12.9	2.5	72.5	37.8
Ortiz-Colberg 1981	L7	1600	1.2	Circular	38.1	38.1	19.1	89.2	41.2	37.7	12.7	12.9	2.5	71.6	37.6
Ortiz-Colberg 1981	L9	991	1.2	Circular	25.4	25.4	12.7	89.2	41.2	37.7	12.7	12.9	2.5	68.9	41.8
Ortiz-Colberg 1981	L10	988	1.2	Circular	38.1	38.1	19.1	89.2	41.2	37.7	12.7	12.9	2.5	66.5	44.9
Ortiz-Colberg 1981	L14	993	1.2	Circular	12.7	12.7	6.4	89.2	41.2	37.7	12.7	12.9	2.5	67.5	42.7
Ortiz-Colberg 1981	L16	1295	1.9	Circular	25.4	25.4	12.7	89.2	41.2	37.7	12.7	12.9	2.5	115.2	76.5
Ortiz-Colberg 1981	L17	1298	1.9	Circular	38.1	38.1	19.1	89.2	41.2	37.7	12.7	12.9	2.5	115.2	66.7
Ortiz-Colberg 1981	L19	686	1.9	Circular	38.1	38.1	19.1	89.2	41.2	37.7	12.7	12.9	2.5	123.3	94.3
Ortiz-Colberg 1981	L22	1143	1.9	Circular	38.1	38.1	19.1	89.2	41.2	37.7	12.7	12.9	2.5	111.8	89.0
Ortiz-Colberg 1981	L26	1143	1.9	Circular	25.4	25.4	12.7	89.2	41.2	37.7	12.7	12.9	2.5	109.7	85.0
Ortiz-Colberg 1981	L27	686	1.9	Circular	25.4	25.4	12.7	89.2	41.2	37.7	12.7	12.9	2.5	115.7	97.4
Ortiz-Colberg 1981	L28	686	1.9	Circular	25.4	25.4	12.7	89.2	41.2	37.7	12.7	12.9	2.5	101.3	99.6
Ortiz-Colberg 1981	L32	1600	1.9	Circular	25.4	25.4	12.7	89.2	41.2	37.7	12.7	12.9	2.5	114.7	59.2